REPORT

Suppression of the *Escherichia coli rnpA49* conditionally lethal phenotype by different compensatory mutations

ARIANNE M. BABINA,[1,3] LEIF A. KIRSEBOM,[2] and DAN I. ANDERSSON[1]

[1]Department of Medical Biochemistry and Microbiology, [2]Department of Cell and Molecular Biology, Uppsala University, 751 23 Uppsala, Sweden

ABSTRACT

RNase P is an essential enzyme found across all domains of life that is responsible for the 5′-end maturation of precursor tRNAs. For decades, numerous studies have sought to elucidate the mechanisms and biochemistry governing RNase P function. However, much remains unknown about the regulation of RNase P expression, the turnover and degradation of the enzyme, and the mechanisms underlying the phenotypes and complementation of specific RNase P mutations, especially in the model bacterium, *Escherichia coli*. In *E. coli*, the temperature-sensitive (ts) *rnpA49* mutation in the protein subunit of RNase P has arguably been one of the most well-studied mutations for examining the enzyme's activity in vivo. Here, we report for the first time naturally occurring temperature-resistant suppressor mutations of *E. coli* strains carrying the *rnpA49* allele. We find that *rnpA49* strains can partially compensate the ts defect via gene amplifications of either RNase P subunit (*rnpA49* or *rnpB*) or by the acquisition of loss-of-function mutations in Lon protease or RNase R. Our results agree with previous plasmid overexpression and gene deletion complementation studies, and importantly suggest the involvement of Lon protease in the degradation and/or regulatory pathway(s) of the mutant protein subunit of RNase P. This work offers novel insights into the behavior and complementation of the *rnpA49* allele in vivo and provides direction for follow-up studies regarding RNase P regulation and turnover in *E. coli*.

Keywords: RNase P; suppressor mutation; Lon; gene amplification; RNase R

INTRODUCTION

RNase P is an ancient and essential endoribonuclease found in Bacteria, Archaea, and Eukaryotes that is responsible for the cleavage of 5′-end leader sequences present on premature tRNA (pre-tRNA) transcripts. Since its discovery in the 1970s, numerous studies have characterized different RNase P variants across diverse model organisms (for reviews, see Kazantsev and Pace 2006; Ellis and Brown 2009; Lai et al. 2010; Klemm et al. 2016; Phan et al. 2021; Jarrous and Liu 2023).

In *Escherichia coli*, as in most other bacteria, RNase P is a heterodimer comprised of a small protein subunit (C5 protein, encoded by *rnpA*) and an RNA subunit (M1 RNA, encoded by *rnpB*) (Harris et al. 1998; Altman and Kirsebom 1999). M1 RNA is the catalytic subunit of the enzyme and plays crucial roles in substrate recognition and C5 folding, intracellular solubility, and proteostasis (Guerrier-Takada et al. 1983; Son et al. 2015), as the bacterial C5 protein behaves as an intrinsically unstructured or natively unfolded protein at low ionic strength (Henkels et al. 2001). The C5 protein is important for M1 RNA metabolic stability and has been implicated in electrostatic shielding, substrate binding, product release, and preventing rebinding of the product (Reich et al. 1988; Tallsjö and Kirsebom 1993; Buck et al. 2005; Sun and Harris 2007; Kim and Lee 2009; Kirsebom and Trobro 2009; Lin et al. 2016). In addition to the 5′-end processing of pre-tRNA, bacterial RNase P is essential for the separation of pre-tRNAs from polycistronic operon transcripts (Mohanty et al. 2020) and is involved in the processing of, for example, 4.5S RNA, among other non-tRNA substrates (for a review focusing on *E. coli*, see Hartmann et al. 2009).

Over the years, many different conditionally lethal mutants and/or inducible complementation systems in the primary bacterial models, *E. coli* and *Bacillus subtilis*, have been used to investigate RNase P assembly and activity in vivo. For example, the temperature-sensitive (ts) mutants

[3]**Present address:** School of Infection and Immunity, University of Glasgow, Glasgow G12 8QQ, United Kingdom

Corresponding author: arianne.babina@imbim.uu.se, arianne.babina@glasgow.ac.uk

Handling editor: Eric Westhof

Article is online at http://www.rnajournal.org/cgi/doi/10.1261/rna.079909.123. Freely available online through the *RNA* Open Access option.

A49, ts241, and ts709, which exhibit defects in $tRNA^{Tyr}Su3$ at higher temperatures, were selected in *E. coli*. These mutants were found to carry changes in the RNase P protein (C5/*rnpA*) and RNA (M1 RNA/*rnpB*) subunits (Schedl and Primakoff 1973; Sakano et al. 1974; Sakamoto et al. 1983; Kirsebom et al. 1988). Conditionally lethal *B. subtilis* mutants in which *rnpA* or *rnpB* expression can be suppressed via inducible promoters have been constructed (Gößringer et al. 2006; Wegscheid et al. 2006; Wegscheid and Hartmann 2007) as well as *E. coli* strains in which the chromosomal *rnpB* gene was either deleted (Waugh and Pace 1990) or under control of an arabinose-dependent promoter (Wegscheid and Hartmann 2006). For growth, these mutants typically depend on the expression of the corresponding functional RNase P subunit from plasmids. For this study, we chose to focus on the ts A49 mutation in *E. coli*, as it was the first RNase P mutant isolated and its mutant phenotype is well-characterized (Schedl and Primakoff 1973; Apirion 1980).

The *E. coli* ts A49 mutation, also known as the *rnpA49* allele, was first isolated from mutagenesis experiments in 1973 and is caused by an A to G transition resulting in the substitution of an arginine to a histidine at position 46 within the C5 protein ($C5^{A49}$) (Schedl and Primakoff 1973; Apirion 1980; Kirsebom et al. 1988). This mutation reduces the solubility of the C5 protein and is hypothesized to impact the association of the C5 protein and M1 RNA subunits to form the RNase P holoenzyme, resulting in reduced RNase P stability and activity (Baer et al. 1989; Li et al. 2003). Strains containing the *rnpA49* allele demonstrate a slight growth defect at permissive temperatures (30°C–33°C) and rapidly accumulate precursor tRNAs and unprocessed polycistronic tRNA transcripts when shifted to the nonpermissive temperature (42°C), eventually leading to arrest of cell growth and death (Schedl and Primakoff 1973; Li et al. 2003; Mohanty and Kushner 2007, 2008; Agrawal et al. 2014).

Previous work has shown that the *E. coli rnpA49* ts phenotype can be complemented by plasmid overexpression of either the wild-type or mutant C5 protein (Vioque et al. 1988; Jovanovic et al. 2002), M1 RNA from *E. coli* (Jain et al. 1982; Motamedi et al. 1984; Baer et al. 1989), or with various C5 protein homologs from other bacterial species (Morse and Schmidt 1992; Pascual and Vioque 1996). Other studies have reported that overexpression of arginine $tRNA_{CCG}$ from both *E. coli* (Kim et al. 1998) and *Brevibacterium albidum* (Kim et al. 1997) can complement the temperature sensitivity caused by the *rnpA49* mutation; however, the mechanism underlying this rescue has not been elucidated. Furthermore, site-directed mutagenesis of the *rnpA49* allele has identified a number of amino acid changes that can compensate the ts defect (Jovanovic et al. 2002), and additional hydroxylamine mutagenesis experiments have led to the identification of compensatory mutations in *rnpB* that can rescue the growth of A49 strains at the nonpermissive temperature (Morse and Schmidt 1993). Lastly, recent work has shown that the deletion of poly(A) polymerase I (PAP I, encoded by *pcnB*) can also partially rescue the ts defect caused by the *rnpA49* allele (Mohanty et al. 2020).

Although these studies provide invaluable insights into RNase P assembly, structure, and function in vivo and demonstrate that there are many ways to rescue the *E. coli rnpA49* ts phenotype, they relied on the use of artificial approaches to examine complementation, such as plasmid overexpression, gene deletions, and mutagenesis. Subsequently, there remains a gap in the literature regarding how *E. coli* can naturally compensate for and suppress the deleterious effects brought about by the *rnpA49* mutation at nonpermissive temperatures. In this work, we isolated and characterized naturally occurring second-site suppressor mutations of the ts phenotype in an *E. coli* strain harboring the *rnpA49* allele. Consistent with past plasmid overexpression studies, we found that *E. coli* can compensate for a defective RNase P by increasing the copy number of either *rnpA49* or *rnpB* via large genome amplifications. We also identified RNase R loss-of-function mutations, as well as numerous mutations impacting Lon protease expression and activity. These latter findings present novel links between the mutant RNase P, RNase R, and Lon protease, setting the stage for further investigations into RNase P regulation, degradation, and turnover in *E. coli*.

RESULTS AND DISCUSSION

Isolation of suppressor mutants that enable the growth of *E. coli* A49 at the nonpermissive temperature

Suppressor mutants of an *E. coli* strain carrying the ts *rnpA49* allele were isolated from standard fluctuation assays performed at the nonpermissive temperature. Briefly, $\sim 10^8$ cells from 40 independent *E. coli* A49 cultures grown at permissive temperature were plated on LB-agar and incubated for 48 h at the nonpermissive temperature (42°C). From these experiments, the mutation rate for *E. coli* A49 ts revertants generated by spontaneous mutation was determined to be $\sim 10^{-10}$ to 10^{-9} per cell per generation using the bz-rates web tool (Gillet-Markowska et al. 2015).

After incubation, a single colony from each plate was randomly selected, restreaked, and retested for growth at 42°C, and then locally sequenced to confirm the retention of the *rnpA49* allele. Seventeen isolates carrying no additional mutations in the *rnpA49* locus were selected for additional Sanger and/or whole-genome sequencing to identify potential second-site suppressor mutations and for further characterization (Fig. 1A; Table 1; Supplemental Table S1). These suppressor isolates were subsequently classified as one of three mutation types, which are discussed in detail below: (i) gene amplifications of *rnpA49* or *rnpB*, (ii)

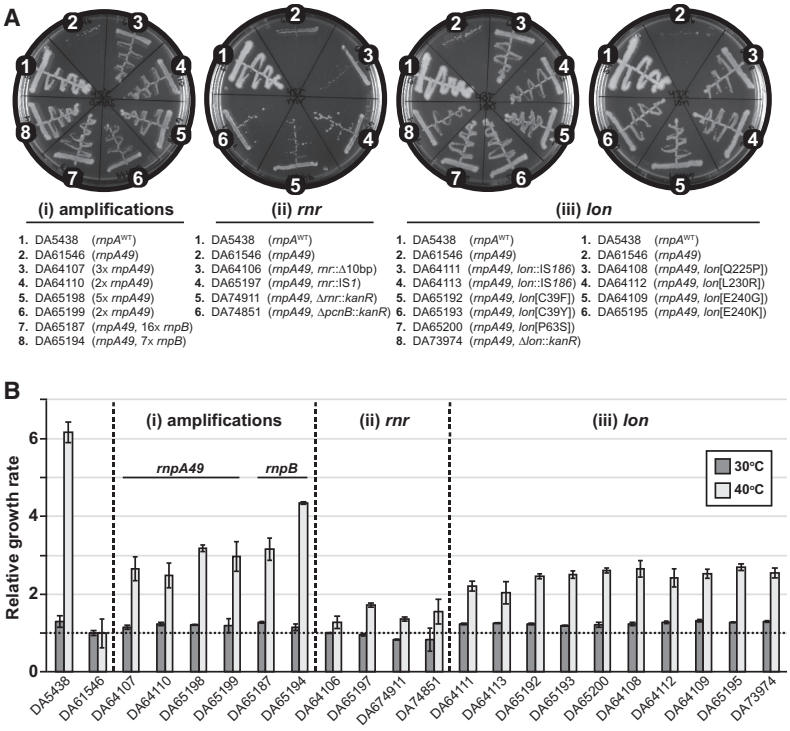

FIGURE 1. Suppressor mutations rescue the growth of *Escherichia coli* A49 at the nonpermissive temperature. (*A*) Growth of the *E. coli* A49 suppressor strains carrying (*i*) amplifications of *rnpA49* or *rnpB* or loss-of-function mutations in (*ii*) *rnr* or (*iii*) *lon* on LB-agar after 24 h incubation at the nonpermissive temperature (42°C). DA5438 is *E. coli* MG1655 carrying the wild-type *rnpA* allele; DA61546 is the *E. coli* A49 parental strain carrying the ts *rnpA49* allele. Additional control strains containing *kanR* deletion cassettes from the KEIO collection in the parental DA61546 A49 background are included for comparison. (*B*) Relative exponential phase growth rates of the *E. coli* A49 suppressor strains and relevant control strains as compared to the DA61546 A49 parental strain (set to 1) at the corresponding temperature. Growth measurements were performed in LB medium at both 30°C (permissive temperature) and 40°C (sublethal temperature). The values reported represent the mean of at least three independent biological replicates (with two technical replicates each); error bars represent the standard deviation of the mean.

mutations in *rnr*, and (iii) mutations in *lon*. To assess the extent of complementation, the relative growth rate of each suppressor strain was determined from growth assays in liquid medium at the permissive temperature (30°C) and at a sublethal temperature (40°C). We chose to perform growth assays at 40°C to enable comparison with the original A49 parental strain, as it was the maximum temperature at which our A49 strain reproducibly grew in liquid medium while still demonstrating a significant growth defect (Fig. 1B; Table 1).

Complementation via gene amplifications of *rnpA49* or *rnpB*

Of the 17 suppressor strains selected for further sequencing and study, four strains (DA64107, DA64110, DA65198, and DA65199) were found to have amplifications of the genomic region containing the *rnpA49* allele, encoding the mutant $C5^{A49}$ RNase P protein subunit, and two strains (DA65187 and DA65194) were found to contain amplifications of the genomic region containing the *rnpB* gene, encoding the M1 RNA subunit of RNase P (Table 1; for a schematic explaining gene amplifications, see Supplemental Fig. S1). The copy number of the amplified units varied among the different isolates, ranging from ~2×–5× for the units containing *rnpA49* and 7×–16× for the units containing *rnpB*, and the size of the amplified chromosomal regions ranged from 29 to 192.5 kbp for the units containing *rnpA49* and 17.2–34.5 kbp for the units containing *rnpB* (Supplemental Table S2). Apart from a synonymous mutation in *lsrA* (predicted to encode the ATP-binding component of an AI-2 ABC transporter) that was found in one suppressor strain with an *rnpA49* amplification (DA64110) and a nonsynonymous mutation in one instance of *insA* (one of the IS*1* elements on the chromosome) in a suppressor strain with an *rnpB* amplification (DA65187), no additional mutations were identified (Table 1; Supplemental Table S1). As is commonly observed for genomic amplifications in bacteria, the boundaries of the majority of the amplified chromosomal units were flanked by regions homologous to transposases or insertion sequences, specifically IS*1* and, in one instance, IS*4* (DA64107). However, no repeat sequences or regions of homology were identified within the breakpoints of the amplified units in one *rnpA49* amplification strain (DA64110), suggesting an alternate recombination mechanism not involving homologous segments (Supplemental Table S2; Tlsty et al. 1984; Reams and Roth 2015; Nicoloff et al. 2019).

In the growth assays in liquid medium, the suppressor strains containing amplifications of either *rnpA49* or *rnpB* demonstrated a slight 1.2-fold increase in growth rate relative to the original A49 parental strain at the permissive temperature. At the sublethal temperature, the strains carrying *rnpA49* amplifications exhibited an ~2.5-fold to threefold increase in relative growth rate, whereas the two strains with *rnpB* amplifications demonstrated a three- to fourfold increase in relative growth rate at 40°C (vs. a sixfold increase in relative growth rate for an *E. coli* strain with the wild-type *rnpA* allele at 40°C, DA5438), indicating partial complementation of the ts phenotype (Fig. 1B).

TABLE 1. Summary of *E. coli* A49 suppressor strains isolated from this study

Strain[a]	Description[a]	Relevant genotype[b]	Other mutations	Mean growth rate (h^{-1}) ± SD[c]		Mucoid at 30°C[d]
				30°C	40°C	
DA5438	*rnpA* (WT)	*rnpA*	–	1.27 ± 0.14	2.24 ± 0.11	–
DA61546	*rnpA49* (A49 parental)	*rnpA49*	–	0.97 ± 0.06	0.39 ± 0.15	–
DA64107	3× *rnpA49*	*rnpA49*, DUP (3737267..3928428)	–	1.11 ± 0.05	1.05 ± 0.12	–
DA64110	2× *rnpA49*	*rnpA49*, DUP (3844972..3918184)	*lsrA*[A451A] (GCA > GCT) (synonymous)	1.20 ± 0.05	0.98 ± 0.12	–
DA65198	5× *rnpA49*	*rnpA49*, DUP (3868817..389802)	–	1.18 ± 0.01	1.25 ± 0.03	–
DA65199	2× *rnpA49*	*rnpA49*, DUP (3804071..3899637)	–	1.17 ± 0.17	1.17 ± 0.15	–
DA65187	16× *rnpB*	*rnpA49*, DUP (3251561..3286079)	*insA*[T24T] (ACT > ACC) (synonymous)	1.24 ± 0.02	1.24 ± 0.11	–
DA65194	7× *rnpB*	*rnpA49*, DUP (3267203..3284424)	–	1.12 ± 0.08	1.71 ± 0.01	–
DA64106	*rnr*::Δ10 bp	*rnpA49*, *rnr*::DEL (4404082..4404091)	–	0.98 ± 0.01	0.51 ± 0.06	–
DA65197	*rnr*::IS*1*	*rnpA49*, *rnr*::IS*1*	*trmA*::IS*186*	0.92 ± 0.02	0.68 ± 0.02	–
DA74911	Δ*rnr*::*kanR* (control)	*rnpA49*, DEL*rnr*::*kanR*	–	0.81 ± 0.01	0.54 ± 0.02	–
DA74851	Δ*pcnB*::*kanR* (control)	*rnpA49*, DEL*pcnB*::*kanR*	–	0.81 ± 0.29	0.61 ± 0.13	–
DA64111	*lon*::IS*186*	*rnpA49*, *lon*::IS*186*	–	1.20 ± 0.02	0.87 ± 0.05	++
DA64113	*lon*::IS*186*	*rnpA49*, *lon*::IS*186*	–	1.22 ± 0.01	0.81 ± 0.11	+
DA65192	*lon*[C39F]	*rnpA49*, *lon*[C39F] (TGT > TTT)	–	1.20 ± 0.01	0.97 ± 0.03	–
DA65193	*lon*[C39Y]	*rnpA49*, *lon*[C39Y] (TGT > TAT)	–	1.16 ± 0.02	0.98 ± 0.04	+
DA65200	*lon*[P63S]	*rnpA49*, *lon*[P63S] (CCG > TCG)	–	1.18 ± 0.06	1.03 ± 0.02	–
DA64108	*lon*[Q225P]	*rnpA49*, *lon*[Q225P] (CAG > CCG)	–	1.20 ± 0.05	1.04 ± 0.09	–
DA64112	*lon*[L230R]	*rnpA49*, *lon*[L230R] (CTG > CGG)	–	1.25 ± 0.03	0.95 ± 0.09	+
DA64109	*lon*[E240G]	*rnpA49*, *lon*[E240G] (GAA > GGA)	–	1.30 ± 0.03	1.00 ± 0.05	++
DA65195	*lon*[E240K]	*rnpA49*, *lon*[E240K] (GAA > AAA)	–	1.25 ± 0.01	1.06 ± 0.03	+
DA73974	Δ*lon*::*kanR* (control)	*rnpA49*, DEL*lon*::*kanR*	–	1.27 ± 0.02	1.00 ± 0.05	+++

[a]DA5438 is *E. coli* MG1655 carrying the wild-type *rnpA* allele; DA61546 is the *E. coli* A49 parental strain carrying the ts *rnpA49* allele. Relevant control strains containing *kanR* deletion cassettes from the KEIO collection in the parental DA61546 A49 background are included for comparison. For strains containing amplifications, the relevant gene and its estimated copy number are given.

[b]"DUP" indicates strains containing genomic amplifications; the genomic coordinates for the boundaries of the amplified units are given. "DEL" indicates strains containing deletions; the genomic coordinates for the boundaries flanking the deletion are given. For complete strain genotypes, see Supplemental Table S1. Genomic coordinates are relative to the *E. coli* MG1655 reference genome (GenBank: U00096.3).

[c]Exponential phase growth rates of each strain in LB medium at both 30°C (permissive temperature) and 40°C (sublethal temperature); the values reported represent the mean of at least three independent biological replicates (with two technical replicates each) ± the standard deviation of the mean.

[d]Not mucoid at 30°C (–) or mucoid at 30°C (+ < ++ < +++), as observed on LB-agar plates after overnight incubation.

The correlation between gene copy number and protein abundance was confirmed via tandem mass tag (TMT)-based proteomics of strain DA65198 (Mosier et al. 2015; Paulo et al. 2016; Zecha et al. 2019; Li et al. 2020). Strain DA65198 carries an estimated 5× amplification of the genomic region containing the *rnpA49* allele and correspondingly exhibited a four- to fivefold increase in the abundance of the mutant $C5^{A49}$ protein relative to the original A49 parental strain (DA61546) (Fig. 2A). These findings are in agreement with past plasmid complementation studies and confirm that increasing expression and/or gene copy number of either *rnpA49* or *rnpB* can rescue the ts defect of *E. coli* A49. As the *rnpA49* mutation is hypothesized to reduce the efficiency with which $C5^{A49}$ assembles with the M1 RNA, overexpression of either subunit of the mutant RNase P heterodimer likely shifts the equilibrium of assembly toward formation of the RNase P holoenzyme. This is also consistent with previous work demonstrating that wild-type *rnpA* overexpression increases the steady-state levels of the RNase P holoenzyme (Wegscheid and Hartmann 2006; Gößringer et al. 2023).

Interestingly, there is no clear linear relationship between complementation efficiency and gene copy number or level of amplification. It is well-established that genome amplifications inherently carry a substantial fitness cost (Nicoloff et al. 2019; Pereira et al. 2021); thus, there are likely tradeoffs between the size of the amplified genomic regions, the degree of overexpression from the genes encoded within the amplified units, and overall cell fitness. For example, the strain carrying the 7× *rnpB* amplification (DA65194) exhibited a greater increase in relative growth rate and subsequent extent of complementation in comparison to the strain carrying the 16× *rnpB* amplification (DA65187) (Fig. 1B). The higher copy number coupled with the larger size of the amplified unit (34.5 kbp for DA65187 vs. 17.2 kbp for DA65194) likely render suppressor strain DA65187 slightly less fit than DA65194 (Supplemental Table S2).

The strains carrying *rnpB* amplifications demonstrated the greatest increase in gene copy number relative to those carrying amplifications of *rnpA49* (maximum 16× for *rnpB* vs. 5× for *rnpA49*). As previous work has shown that high-level overexpression of C5 protein is toxic to *E. coli* (Jovanovic et al. 2002), perhaps there is an upper limit to which the *rnpA49* allele can be amplified before the toxicity of $C5^{A49}$ overexpression outweighs complementation of the ts phenotype at the nonpermissive or sublethal temperature. Furthermore, the sizes of the amplified chromosomal units in the two *rnpB* amplification strains were on average smaller than those found in the strains containing the *rnpA49* amplifications (Supplemental Table S2). Therefore, the smaller size of the amplified units may also contribute to the average higher increase in gene copy number observed with the *rnpB* amplification strains. It would be interesting to examine the extent to which subsequent evolution experiments would improve strain growth at the nonpermissive temperature via further amplification, and/or whether the amplifications would eventually be reduced or lost upon accumulation of additional suppressor mutations.

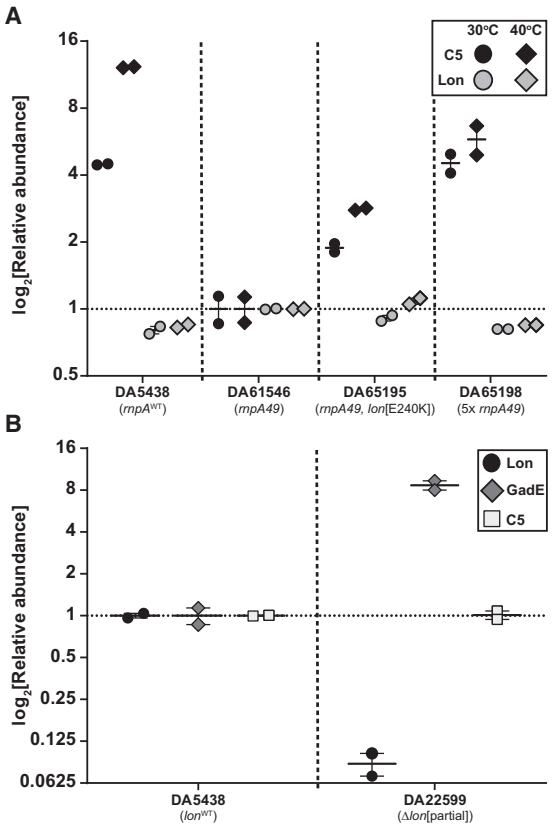

FIGURE 2. Select suppressor mutations increase $C5^{A49}$ protein abundance. (*A*) Relative abundance of either the wild-type or mutant C5 protein and Lon protease during early-to-mid exponential phase growth at the permissive (30°C) or sublethal temperature (40°C), as compared to the original A49 parental strain (DA61546, set to 1). Strains DA61546, DA65195, and DA65198 carry the *rnpA49* mutant allele (encoding $C5^{A49}$). (*B*) Relative abundances of the wild-type C5 protein and Lon protease in *lon*+ (DA5438) and *lon*− (DA22599) *E. coli* MG1655 strains during early-to-mid exponential phase growth at 30°C, as compared to the *E. coli* MG1655 wild-type control strain (DA5438, set to 1). Strain DA22599 contains a partial deletion of the *lon* coding region in an *E. coli* MG1655 genetic background such that the overlapping coding region for the small RNA SraA and the overlapping promoter for the downstream *hupB* gene remain intact (Nicoloff and Andersson 2013). GadE, a known Lon substrate, is included as a control to demonstrate the loss of Lon activity in DA22599 (Heuveling et al. 2008). For both *A* and *B*, total proteome analysis was performed via TMT-based relative quantification using two biological replicates for each strain (at each temperature for *A*). Briefly, peptides isolated from each sample were labeled with unique isobaric TMT tags, pooled, and analyzed using mass spectrometry. Peptides were identified by matching the resulting ion peaks with those reported in fragment databases and relative peptide abundance was quantified by comparing TMT reporter ion intensities across all samples. Horizontal bars represent the mean between the two biological replicates; vertical I-bars represent the range. Some data points overlap.

Complementation via loss-of-function mutations in *rnr*

Two suppressor strains were found to have loss-of-function mutations in *rnr*, encoding RNase R, a 3′–5′ exoribonuclease that is involved in rRNA and tmRNA maturation and turnover, as well as the degradation of polyadenylated RNAs (Andrade et al. 2009; Condon et al. 2021). One suppressor strain (DA64106) contained a 10 bp deletion in the sequence encoding the N terminus of RNase R, resulting in a +1 frameshift after codon 59. The other strain (DA65197) contained an IS*1* insertion in *rnr*, as well as an IS*186* insertion in *trmA*, which encodes a tRNA methyltransferase that also acts as a tRNA chaperone facilitating tRNA folding (Table 1; Supplemental Table S3; Supplemental Fig. S2).

Of all the suppressor mutants isolated, the two strains carrying *rnr* mutations exhibited the weakest complementation of the ts phenotype, with smaller colonies on plates incubated at the nonpermissive temperature and slower growth rates in liquid culture (Fig. 1). Both *rnr* suppressor strains grew comparable to the A49 parental strain at 30°C and exhibited only a modest 1.5-fold increase in growth rate relative to the parental A49 strain at 40°C, the sublethal temperature assayed.

To further confirm that *rnr* loss-of-function mutations can complement the ts phenotype, we generated and assayed the growth of an A49 strain containing the Δ*rnr*::*kanR* deletion cassette from the KEIO collection (DA74911) (Baba et al. 2006). Although this deletion strain grew slower than the original A49 parental strain at the permissive temperature, it grew similarly to the two *rnr* suppressor strains recovered from our screen at the sublethal temperature (Fig. 1B; Table 1). The growth defect of the Δ*rnr*::*kanR* control strain at 30°C may be due to fitness costs associated with a full deletion of *rnr* and the subsequent disruption of the genetic context surrounding the *rnr* open reading frame (ORF), constitutive expression of the *kanR* cassette, and/or disruption to other pathways regulated by RNase R. Additionally, previous studies have shown that *rnr* mutants exhibit growth defects at both standard (i.e., 37°C) and lower temperatures (Cairrão et al. 2003).

It is possible that the *rnr* loss-of-function mutations act via the same complementation mechanism/pathway as the *pcnB* (PAP I) deletion described by Mohanty et al. (2020). Because RNase P function is compromised with the *rnpA49* allele, 5′-unprocessed pre-tRNA transcripts accumulate and become substrates for 3′-end polyadenylation by PAP I, which destabilizes the available pre-tRNA pool and exacerbates the ts growth defect. Deleting PAP I facilitates the accessibility of pre-tRNA 3′-ends for further processing, and studies have shown that the majority of pre-tRNAs that retain their 5′-leaders (i.e., because of a defective RNase P) but have mature 3′-ends are sufficient substrates for aminoacylation (Mohanty et al. 2020). Thus, the absence of *pcnB* ultimately improves the processing and/or aminoacylation of pre-tRNAs to promote survival at the nonpermissive temperature.

Alternatively, it is also possible that RNase R is involved in the turnover and degradation of M1 RNA, as the preprocessed primary M1 RNA transcript is subject to PAP I-mediated poly(A)-dependent degradation (Kim et al. 2005). Thus, the inactivation of *rnr* may directly improve the assembly and stability of the mutant RNase P holoenzyme at the nonpermissive temperature. To investigate whether inactivation of *rnr* improves mutant RNase P stability and/or abundance, we quantified M1 RNA transcript and $C5^{A49}$ protein levels in *rnr* mutant suppressor strain DA65197 (*rnr*::IS*1*) during early-to-mid exponential phase growth at both the permissive (30°C) and sublethal temperature (40°C) using RT-qPCR and mass spectrometry-based proteomics, respectively. Although we observed a very slight increase (1.3-fold) in $C5^{A49}$ protein relative abundance at 40°C (Supplemental Fig. S3), we measured a modest, but not statistically significant decrease in M1 RNA transcript levels in DA65197 at the sublethal temperature relative to the DA61546 A49 parental strain (Supplemental Fig. S4), suggesting that RNase R may not be directly involved in M1 RNA stability and/or degradation. However, follow-up experiments outside the scope of this study are necessary to confirm this postulation. Although RNase E is involved in M1 RNA maturation (Lundberg and Altman 1995; Ko et al. 2008), and studies have shown that the mature M1 RNA is metabolically stable and that association with the C5 protein is required for this stability (Jain et al. 1982; Kim and Lee 2009), the full suite of enzymes involved in M1 RNA turnover in *E. coli* is still unknown.

Lastly, connections between the RNase R and PAP I-mediated poly(A)-dependent degradation pathways and the roles disruptions to these pathways play in suppressing the *rnpA49* ts phenotype are further supported by the fact that our A49 parental strain containing the Δ*pcnB*::*kanR* deletion cassette from the KEIO collection (DA74851) behaves similarly to both the naturally occurring *rnr* suppressor mutants isolated from our screen and the constructed A49 Δ*rnr*::*kanR* control strain at the sublethal temperature (Fig. 1). Like the Δ*rnr*::*kanR* strain, the Δ*pcnB*::*kanR* strain also exhibits a slight growth defect at the permissive temperature relative to the parental A49 strain. Again, this defect may be due to costs associated with *kanR* expression, potential disruption of the regulatory sequences surrounding or overlapping the fully deleted *pcnB* ORF, and/or disruption of other regulatory pathways involving PAP I.

Complementation via promoter disruption and nonsynonymous mutations in *lon*

The majority of mutations recovered from our fluctuation assays affected *lon*, encoding the ATP-dependent AAA+ protease, Lon. In bacteria, Lon is a global regulator that coordinates a number of important processes such as stress

response, DNA replication and repair, and virulence via the degradation of misfolded proteins, rapid turnover of key regulatory proteins, and, in some instances, acting as a protein-folding chaperone (Tsilibaris et al. 2006; Van Melderen and Aertsen 2009; Gur 2013). In *E. coli*, Lon subunits equilibrate between hexamers and dodecamers under physiological conditions (Wohlever et al. 2013). Two strains were found to have an IS*186* insertion in the *lon* promoter region and seven strains were found to contain SNPs resulting in nonsynonymous mutations in the *lon* protein-coding region. Six of the nine *lon* mutant suppressor strains were mucoid when grown at 30°C (DA64109, DA64111, DA64112, DA64113, DA65193, and DA65195), a characteristic phenotype of *E. coli lon* mutants (Table 1; Supplemental Fig. S5; Bush and Markovitz 1973).

Previous studies have shown that the *lon* promoter is a hotspot for IS*186* insertion and that IS*186*-mediated *lon* promoter disruption is a fairly frequent mutation that inhibits *lon* expression under specific selective conditions, such as in the presence of certain antibiotics (Supplemental Table S3; SaiSree et al. 2001; Nicoloff et al. 2007; Nicoloff and Andersson 2013). The *lon*::IS*186* suppressor strains demonstrated an ∼1.3-fold increase in relative growth rate at 30°C, and a twofold increase in relative growth rate at the sublethal 40°C when compared to the original A49 parental strain (Fig. 1B).

Similarly, the suppressor strains carrying the nonsynonymous changes in the *lon* protein-coding sequence also exhibited a 1.3-fold increase in relative growth rate at the permissive temperature. However, these strains complemented the ts defect slightly better than the *lon*::IS*186* suppressor strains, with an average 2.6-fold increase in relative growth rate at the sublethal temperature. Of the seven *lon* protein-coding mutants isolated, four strains contained substitutions at or near residue E240 (Table 1). The E240K mutation has previously been shown to favor Lon's dodecamer conformation and affects substrate recognition and degradation activity. Furthermore, the region surrounding residue 240 has been implicated in substrate recognition and activation of Lon's protease and ATPase activity (Ebel et al. 1999; Cheng et al. 2012; Wohlever et al. 2013). This finding suggests that the suppressor mutants carrying single nonsynonymous mutations within this region (DA64108: Q225P, DA64112: L230R, DA64109: E240G, and DA65195: E240K) likely express a Lon protein with partial or complete loss of function. It is less clear how the suppressor mutations located closer to the N terminus (DA65192: C39F, DA65193: C39Y, and DA65200: P63S) might affect Lon expression and/or function. Although nonsynonymous mutations can directly impact protein function and assembly (as described above), mutations near the 5′-end of a protein-coding gene can also have significant effects on mRNA stability, as well as transcription and/or translation initiation and efficiency (Meyer 2017). Nevertheless, these three suppressor strains behave similar to the isolated *lon* suppressor strains that carry mutations known to alter Lon expression (*lon*::IS*186* promoter disruptions) and function (nonsynonymous mutations surrounding residue 240), and the suppressor strain with the C39Y mutation (DA65193) is mucoid at 30°C, indicating that nonsynonymous mutations close to the N terminus can indeed impact Lon expression and/or activity. Lastly, a control A49 strain containing the Δ*lon*::*kanR* deletion cassette from the KEIO collection (DA73974) was constructed and assayed, confirming that loss of Lon function can partially complement the ts defect caused by the *rnpA49* allele (Fig. 1).

To our knowledge, the wild-type C5 protein subunit of RNase P has not yet been identified as a substrate for Lon protease (Heuveling et al. 2008), and the observation that the abundance of the wild-type C5 protein is similar in *lon*+ (DA5438) and *lon*− (DA22599) *E. coli* MG1655 strains supports this (Fig. 2B). However, it is possible that the mutant $C5^{A49}$ protein is degraded by Lon. Thus, *lon* loss-of-function mutations would stabilize $C5^{A49}$ levels and the overall mutant RNase P holoenzyme to partially suppress the *rnpA49* temperature sensitivity.

To investigate how Lon protease loss-of-function mutations impact the relative abundance of both the wild-type and mutant C5 protein, we performed total proteome analysis on select *E. coli* strains during early-to-mid exponential phase growth at both the permissive (30°C) and sublethal temperatures (40°C) (Fig. 2A). Although relative abundances of the mutant Lon[E240K] protein and M1 RNA transcript in suppressor strain DA65195 remained similar to those of both the A49 parental strain (DA61546) and the MG1655 wild-type strain (DA5438) (Fig. 2A; Supplemental Fig. S4), suppressor strain DA65195 demonstrated an approximately two- to threefold increase in the relative abundance of the mutant $C5^{A49}$ protein subunit as compared to the original ts A49 parental strain (Fig. 2A). This increase in $C5^{A49}$ protein abundance coincides with the almost threefold increase in the suppressor strain's relative growth rate at the nonpermissive temperature (Fig. 1) and indicates that the mutant $C5^{A49}$ protein is potentially a substrate of Lon protease.

This observation is consistent with findings from a similar study in which a mutant RNA polymerase σ subunit was found to be a direct substrate for Lon proteolysis and *lon* loss-of-function mutations suppressed the ts phenotype caused by the mutant *rpoD800* allele (Grossman et al. 1983). Moreover, recent work suggests that Lon-mediated proteolysis may serve as a quality control measure to prevent the accumulation of nonfunctional RNA-binding proteins (RBPs). In particular, RNA-binding deficient mutants of ProQ and Hfq, the two major RBPs facilitating sRNA activity in bacteria, have been found to be targets of Lon degradation in *Salmonella* (El Mouali et al. 2021). Although naturally occurring *lon* loss-of-function mutations were not characterized in this study, the ProQ and Hfq mutants demonstrated increased stability and/or abundance in Δ*lon* genetic backgrounds. Unlike the A49 suppressor strains

carrying *lon* mutations, the mutant phenotypes of the ProQ- and Hfq-deficient strains could not be rescued by increasing the abundance of the mutant proteins, as the mutations directly impacted protein function rather than protein complex or holoenzyme assembly. Regardless, the present study potentially adds the *E. coli* C5 protein to the list of bacterial RBPs regulated by Lon-mediated quality control mechanisms.

Previous work demonstrating that M1 RNA acts as a chaperone to facilitate C5 protein folding, solubility, and stability further supports our proposed Lon-mediated degradation model (Son et al. 2015). When the C5 protein is misfolded or mutated (as is the case with the *rnpA49* mutant allele), Son et al. found that weakened interactions with M1 RNA are sufficient to prevent aggregation of otherwise insoluble mutant C5 proteins and facilitate their proteolytic degradation. Investigations of this hypothesis in a *lon*-deficient strain of *E. coli* showed that mutant C5 proteins aggregated in the presence of M1 RNA. It is possible that this increased aggregation also indicates increased mutant C5 protein abundance because of the *lon* deletion, reinforcing our findings that suggest mutant C5 proteins are potentially targets for Lon-dependent proteolysis.

Because of its role as a chaperone and global regulator, it is also possible that Lon indirectly impacts $C5^{A49}$ protein stability via the regulation of other proteases and/or pathways. Nevertheless, our understanding of RNase P metabolism in *E. coli* remains incomplete, and additional studies are required to further elucidate the pathways and mechanisms involved in regulating *E. coli* RNase P levels.

Concluding remarks

In this study, we report for the first time naturally occurring second-site compensatory mutations of the *rnpA49* ts phenotype in *E. coli*. Although a relatively small screen, similar mutations were recovered multiple independent times across the 17 suppressor strains isolated, suggesting that these are frequent targets for compensatory evolution (Fig. 3). The compensatory mechanisms underlying the genomic amplifications of the regions containing the genes encoding either subunit of the mutant RNase P complex are well-established from past plasmid overexpression studies, and there is precedent for the role of RNase R loss-of-function mutations in the literature. However, follow-up studies are necessary to determine the exact mechanism behind the *rnr* suppressor mutations. Additionally, we found that *E. coli* frequently suppresses the ts defect caused by the *rnpA49* allele via mutations that likely inactivate or alter the activity or expression of Lon protease and that select suppressor strains with *lon* mutations have increased $C5^{A49}$ protein abundance. This finding suggests that the mutant $C5^{A49}$ protein is potentially a substrate for Lon degradation and/or Lon protease is indirectly involved in the regulation of $C5^{A49}$ protein levels. Previous work indicates that Lon protease plays a role in bacterial RBP quality control by specifically degrading mutant and/or nonfunctional RBPs and not their wild-type counterparts. Again, additional investigations are needed to understand Lon's role in RNase P metabolism in greater detail.

Although the isolated strains grow comparable to wild-type *E. coli* (DA5438) at the permissive temperature, the suppressor mutations only partially complement the ts

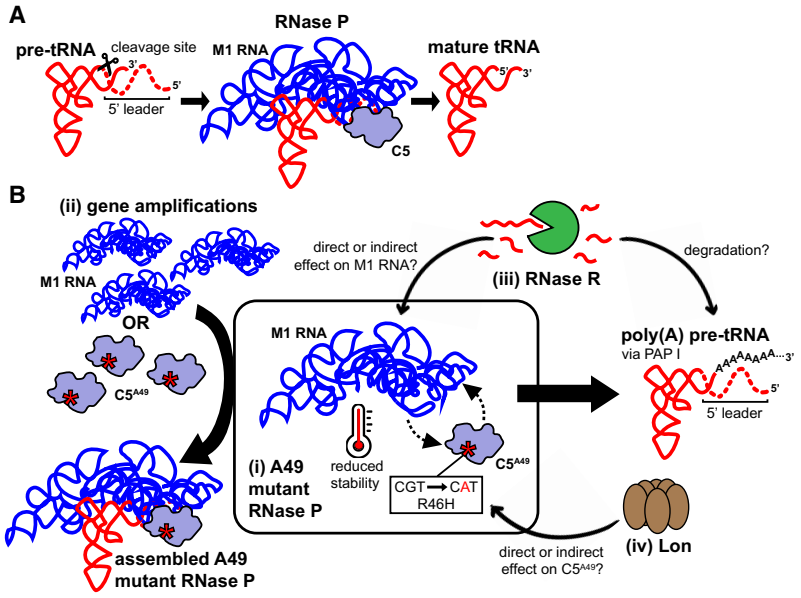

FIGURE 3. Schematic summary of the *E. coli* A49 second-site suppressor mutations isolated from this study. (*A*) Among other roles, RNase P is responsible for the 5′-end maturation of tRNAs by cleaving the 5′ leader sequences found on pre-tRNA transcripts. In *E. coli* strains carrying the wild-type *rnpA* allele, the C5 protein and M1 RNA subunits readily assemble to form the functional holoenzyme. (*B*) (i) The *rnpA49* mutant allele encodes a ts mutation that compromises the assembly and stability of the RNase P holoenzyme at nonpermissive temperatures. This leads to an accumulation of pre-tRNAs with unprocessed 5′-ends, which are often polyadenylated by PAP I and targeted for degradation. (*ii*) The *rnpA49* ts phenotype can be partially suppressed by increasing the gene copy number of either subunit of the mutant RNase P complex (*rnpA49* or *rnpB*) via large genome amplifications, which shifts the equilibrium of assembly to favor the formation of the mutant RNase P holoenzyme. (iii) Rescue of the *rnpA49* ts phenotype can also occur via the acquisition of loss-of-function mutations in RNase R. RNase R targets polyadenylated RNAs for degradation, thus inactivation of RNase R likely stabilizes the unprocessed, polyadenylated pre-tRNAs for aminoacylation and/or may also contribute to increased M1 RNA stability and improved assembly of the mutant RNase P holoenzyme. (iv) Lastly, *rnpA49* suppressor mutations inactivating Lon protease increase $C5^{A49}$ protein abundance to promote mutant RNase P holoenzyme assembly and stability.

phenotype at the sublethal and nonpermissive temperatures, and growth rates are not restored to wild-type levels at the higher temperatures. This can potentially be attributed to the inherent costs of the suppressor mutations themselves. As mentioned previously, large genome amplifications can have substantial impacts on cell fitness (Nicoloff et al. 2019; Pereira et al. 2021), high-level C5 protein overexpression is known to be toxic to *E. coli* (Jovanovic et al. 2002), and the disruption of the various regulatory functions of RNase R and Lon likely have off-target effects on overall fitness. Furthermore, only single relevant suppressor mutations were identified in each strain. Therefore, it is possible that additional mutations could arise with subsequent evolution experiments to more fully complement the ts defect and/or compensate for the fitness costs brought about by the original suppressor mutations.

Apart from the overexpression of either RNase P subunit via genome amplifications, the other second-site suppressor mutations recovered were loss-of-function mutations in other enzymes, suggesting that there is no promiscuous and/or moonlighting activity from alternative *E. coli* RNases or other proteins that can compensate for the mutant RNase P. To determine if the overexpression of other *E. coli* ORFs can in fact rescue the *rnpA49* ts defect, we introduced a plasmid library containing pooled clones from the ASKA collection (representing 4000 cloned ORFs from *E. coli*) into our *E. coli* A49 strain and screened for ORFs that could enable strain growth at the nonpermissive temperature (42°C) (Kitagawa et al. 2006). The gene encoding the wild-type C5 protein, *rnpA*, was the only "positive hit" recovered from this screen, further supporting our observation that complementation is primarily driven by overexpression of RNase P or loss-of-function mutations in other genes, rather than via gain-of-function mutations and/or increased expression of other potentially promiscuous enzymes (Supplemental Fig. S6).

It is worth noting that ts mutant strains may have phenotypes that are not directly linked to the function, regulation, and metabolism of the wild-type enzyme, as functional complementation studies need to be performed under temperature stress conditions, which can globally effect gene expression and exacerbate the mutant phenotype (Li et al. 2003). For example, the proposed role of yeast RNase P in the maturation of box C/D small nucleolar RNAs was initially identified in a yeast ts strain (Coughlin et al. 2008); however, this phenotype was not observed in a yeast RNase P RNA deletion strain complemented with an eukaryotic protein-only form of RNase P (PRORP) under conditions of normal temperature growth (Weber et al. 2014). This may also be the case with our observation that Lon protease is involved in regulating $C5^{A49}$ protein abundance but has no effect on wild-type C5 protein levels. Nevertheless, recent work suggests that Lon protease might act on mutant RBPs as a quality control measure in bacteria; therefore, targeting mutant C5 protein variants for Lon-dependent degradation might be an innate control measure that is also found in wild-type *E. coli* genetic backgrounds (El Mouali et al. 2021). In addition, past studies with the ts A49 strain have revealed previously unknown RNase P substrates and functional connections between RNase P and different metabolic pathways (Li et al. 2003). Thus, despite the aforementioned caveats, investigations using ts strains can provide invaluable insights that can inform routes for further investigation in wild-type genetic settings and/or under more standard or relevant growth conditions.

For decades, the molecular, biochemical, and structural elements governing RNase P function have been the subject of hundreds of studies across different organisms. Nevertheless, the regulation of RNase P expression, its turnover and degradation, and the mechanisms underlying certain RNase P mutations are still not fully understood, especially in *E. coli*. Although informative, previous efforts to examine the suppression of the *E. coli rnpA49* ts phenotype have been limited to "artificial" plasmid overexpression, gene deletion, and mutagenesis approaches. Our work complements these past studies and describes new mechanisms by which *E. coli* A49 could naturally compensate for the RNase P assembly and fitness defects caused by the mutant *rnpA49* allele. All of the suppressor mutations isolated from our study appear to favor the formation and stability of the mutant RNase P holoenzyme (*rnpA49* and *rnpB* amplifications, *lon* mutations) or the stability of the enzyme's pre-tRNA substrates (*rnr* mutations) to ultimately improve cell survival at the nonpermissive temperature. Our findings suggest novel links between *E. coli* RNase P and the regulatory pathways involving RNase R and Lon protease and implicate the mutant $C5^{A49}$ RNase P protein subunit as a potential target for Lon proteolysis. This work provides direction for future investigations into RNase P regulation and metabolism in *E. coli*, especially in more wild-type genetic contexts and conditions.

MATERIALS AND METHODS

Bacterial strains and growth conditions

The ts *rnpA49* allele was transferred from the original mutagenized *E. coli* A49 strain [*E. coli* Genetic Stock Center Strain 6465; Strain Designation N2020; F-, *lacZ8*(Am), *trpA36*, *glyA34*, *argA52*, *rpsL999*(*strR*), *rnpA49*(ts), *ilvG866*(Act)] (Apirion 1980) to an *E. coli* MG1655 background (F-, λ-, *rph-1*) using P1 transduction (Thomason et al. 2007). The presence of the ts mutation of interest was confirmed via lack of growth at the nonpermissive temperature (42°C) and local and whole-genome sequencing (MG1655 A49 strain designated as DA61546). For all experiments, strains were grown in lysogeny broth (LB Miller; 10 g/L NaCl, 10 g/L tryptone, 5 g/L yeast extract; Sigma-Aldrich) or plated on LB supplemented with 1.5% (w/v) agar (LB-agar; Millipore). All strains generated in this study were cryo-preserved at −80°C in LB supplemented with 10% DMSO. A49 strains containing additional gene deletions were constructed by P1 transduction of the *kanR* cassette from the

corresponding KEIO collection strain and selection on LB-agar supplemented with 50 µg/mL kanamycin at 30°C (Baba et al. 2006; Thomason et al. 2007). See Supplemental Table S1 for the list of strains used, isolated, and/or constructed for this study.

Fluctuation assays

Twenty cultures of *E. coli* A49 strain DA61546 inoculated from independent colonies were grown overnight in 1 mL LB at 30°C with shaking at 190 rpm. To confirm the amounts of cells to be plated (see below), serial dilutions of each overnight culture were plated on LB-agar and incubated overnight at 30°C, and colonies were counted. For the fluctuation assay, ~10^8 cells (50 µL) from each overnight culture were plated on LB-agar prewarmed to 42°C, and then incubated at 42°C (nonpermissive temperature) for a total of 48 h. Plates were monitored and colonies were counted after 16, 20, and 48 h incubation. After 48 h, a single colony was randomly chosen from each plate with growth, reisolated on LB-agar plates incubated at 30°C, retested for growth at 42°C, and saved for future studies. Mutation rate was determined using the bz-rates webtool, which implements the Ma–Sandri–Sakar maximum likelihood estimator (Hamon and Ycart 2012; Gillet-Markowska et al. 2015). This experiment was performed independently twice, for a total of 40 independent colonies from A49 strain DA61546 being assayed.

Whole-genome sequencing

Before whole-genome sequencing, the *rnpA49* and *lon* loci of select ts revertant strains isolated from the fluctuation assays were PCR-amplified and Sanger sequenced (Eurofins) to confirm the presence of the *rnpA49* and wild-type *lon* alleles (see Supplemental Table S4 for the list of oligos used for PCR and local sequencing). These strains were then grown for whole-genome sequencing in 1 mL LB medium overnight at 30°C with shaking at 190 rpm. Genomic DNA was extracted from 0.5 mL of each culture using an Epicentre MasterPure Complete DNA and RNA Purification Kit according to the manufacturer's protocol. DNA was resuspended in nuclease-free water (Sigma), concentrations were determined using a Nanodrop 1000 (Thermo Scientific) and Qubit 2.0 fluorometer (DNA Broad-Range kit, Invitrogen), and sequencing was performed in-house using an Illumina MiSeq platform with a Nextera XT DNA library preparation kit. Sequences were mapped to the *E. coli* MG1655 reference genome (GenBank U00096.3) and mutations were identified using CLC Genomic Workbench software (QIAGEN). The extent of DNA amplification was estimated by dividing the average sequence coverage of the amplifications by the average sequence coverage of the rest of the chromosome in CLC Genomic Workbench (QIAGEN) as described previously (Nicoloff et al. 2019). All raw sequence reads for the whole-genome sequencing from this study are deposited in the Sequence Read Archive (SRA) at the National Center for Biotechnology Information (NCBI) under BioProject Accession PRJNA1032291.

Growth assays

Growth curves were obtained using a Bioscreen C instrument (Oy Growth Curves AB, Ltd.). Overnight cultures (1 mL LB) of select strains were grown in triplicate from independent colonies at 30°C with shaking at 190 rpm and used to inoculate 1 mL fresh LB cultures (1 µL, 1:1000 dilution). From this dilution, two 300 µL aliquots were transferred to Bioscreen C honeycomb plates to serve as technical replicates. Plates were incubated in the Bioscreen C for 24 h (30°C assays, permissive temperature) or 4 days (40°C assays, sublethal temperature) with shaking, and the OD_{600} was measured every 4 min. The background OD_{600} measurements from wells containing blank, uninoculated medium were subtracted from the OD_{600} measurements. Growth rates were calculated from the linear slope of $\ln(OD_{600})$ during the exponential phase [$\ln(OD_{600}) = -3.5$ to -2.5], and the relative growth rate was calculated by dividing the growth rate of each suppressor or control strain by that of the parental A49 strain (DA61546) in the corresponding condition. The reported values represent the mean of at least three biological replicates, with two technical replicates each; the reported error is the standard deviation of the mean.

Proteomics sample preparation

Cultures (5 mL LB) started from two or three independent colonies from select suppressor and control strains were grown overnight at 30°C with shaking (190 rpm). These were used to inoculate two 500 mL flasks containing 60 mL LB to a starting OD_{600} of ~0.06. For each strain/biological replicate, one flask was incubated at 30°C with shaking (190 rpm) and one flask was incubated at 40°C (water bath) with shaking (175 rpm), until an OD_{600} ~0.2–0.25 was reached. Flasks were then cooled on ice for 10–20 min, cells were pelleted at 4500 rpm, 15 min at 4°C, washed twice with 1 mL phosphate-buffered saline (PBS; 8 g/L NaCl, 0.2 g/L KCl, 1.44 g/L Na_2HPO_4, and 0.24 g/L KH_2PO_4), and then stored at −80°C until proteomics experiments were performed.

The bacterial samples were homogenized by bead-beating using a FastPrep-24 instrument (MP Biomedicals) in SDS buffer, and protein concentration was determined using Pierce BCA Protein Assay Kit (Thermo Scientific) on a SpectraMax iD3 (Molecular Devices). Proteins were reduced in 10 mM dithiothreitol at 56°C for 30 min, then alkylated with 20 mM chloroacetamide at room temperature for 10 min. Protein samples were added to washed hydrophobic and hydrophilic Sera-Mag SpeedBeads (Carboxylate-Modified, Cytiva) in a bead-to-protein ratio of 10:1. The SP3 workflow was adapted from the protein and peptide cleanup for mass spectrometry protocol provided by the manufacturer. In short, proteins were precipitated on the beads by acetonitrile, washed with ethanol, and dried at room temperature. For digestion, 50 mM TEAB and LysC+trypsin (Promega) were added in a protein-to-enzyme ratio of 100:1, and incubation took place overnight at 37°C while shaking. An additional portion of trypsin (Thermo Fisher Scientific) was added and digested for 3 h. The peptide concentration was determined, and aliquots of 30 µg peptides were labeled in 100 mM TEAB using TMTpro 18-plex isobaric mass tagging reagents (Thermo Fisher Scientific) according to the manufacturer's instructions. Samples were pooled into one TMT-set each, and peptides were purified using a HiPPR detergent removal kit and Pierce peptide desalting spin columns (both Thermo Fisher Scientific), according to the manufacturer's instructions. The TMT-sets were fractionated by basic reversed-phase chromatography using a Dionex Ultimate 3000 UPLC system (Thermo Fisher Scientific). Peptide separations were performed using a reversed-phase XBridge BEH C18 column (3.5 µm, 3.0 × 250 mm, Waters

Corporation) and a stepped gradient from 3% to 54% solvent B over 65 min followed by an increase to 80% solvent B at a flow of 200 µL/min. Solvent A was 25 mM ammonia and solvent B was 84% acetonitrile. The 96 primary fractions were combined into 15 final fractions, which were evaporated and reconstituted in 3% acetonitrile and 0.1% trifluoroacetic acid for LC-MS3 analysis.

LC-MS3 analysis

The above fractions were analyzed on an Orbitrap Eclipse Tribrid mass spectrometer equipped with the FAIMS Pro ion mobility system and interfaced with an Easy-nLC1200 liquid chromatography system (both Thermo Fisher Scientific). Peptides were trapped on an Acclaim Pepmap 100 C18 trap column (100 µm × 2 cm, particle size 5 µm, Thermo Fisher Scientific) and separated on an in-house packed analytical column (39 cm × 75 µm, particle size 3 µm, Reprosil-Pur C18, Dr. Maisch) using a stepped gradient from 4% to 80% acetonitrile in 0.2% formic acid over 75 min at a flow of 300 nL/min. FAIMS Pro was alternating between the compensation voltages (CVs) of −50 and −70, and the same data-dependent settings were used at both CVs. The precursor ion mass spectra were acquired at a resolution of 120,000 and an *m/z* range of 375–1500. Using a cycle time of 1.5 sec, the most abundant precursors with charges 2–7 were isolated with an *m/z* window of 0.7 and fragmented by collision-induced dissociation (CID) at 30%. Fragment spectra were recorded in the ion trap at a Rapid-Scan rate. The 10 most abundant MS2 fragment ions were isolated using multinotch isolation for further MS3 fractionation. MS3 fractionation was performed using higher-energy collision dissociation (HCD) at 55%, and the MS3 spectra were recorded in the Orbitrap at 50,000 resolution and an *m/z* range of 100–500.

Proteomic data analysis

Identification and relative quantification were performed using Proteome Discoverer (Thermo Fisher Scientific). The data were matched against the *E. coli* SwissProt database (5385 entries, May 2023). Database matching was performed using SEQUEST as a search engine with a precursor tolerance of 5 ppm and a fragment ion tolerance of 0.6 Da. Tryptic peptides were accepted with one missed cleavage; methionine oxidation was set as a variable modification and cysteine carbamidomethylation, TMTpro on lysine, and peptide N termini were set as fixed modifications. Percolator was used for PSM validation with a strict FDR threshold of 1%. For quantification, TMT reporter ions were identified in the MS3 HCD spectra with 3 mmu mass tolerance, and the TMT reporter intensity values for each sample were normalized on the total peptide amount. The SPS Mass Match threshold was set to 65%, and a SEQUEST XCorr threshold score of 2 was chosen. Only unique peptides were used for relative quantification, and proteins were required to pass a protein FDR of 5%. The mass spectrometry proteomics data have been deposited to the ProteomeXchange Consortium via the PRIDE partner repository with the data set identifier PXD047498 (Perez-Riverol et al. 2019). For the experiments using three biological replicates, the relative abundance of select proteins from select A49 suppressor strains was compared to that of the DA61546 A49 parental strain at the corresponding temperature using a two-tailed Mann–Whitney test in GraphPad Prism. Values were considered significantly different if $P < 0.05$.

RT-qPCR

As above, cultures (5 mL LB) started from three independent colonies from select suppressor and control strains were grown overnight at 30°C with shaking (190 rpm). These were used to inoculate two 500 mL flasks containing 60 mL LB to a starting OD_{600} of ∼0.06. For each strain/biological replicate, one flask was incubated at 30°C with shaking (190 rpm) and one flask was incubated at 40°C (water bath) with shaking (175 rpm), until an OD_{600} of ∼0.2–0.25 was reached. Flasks were then cooled on ice for 10–20 min, and 0.5 mL aliquots of each culture were combined with 1 mL RNAprotect Reagent (QIAGEN), incubated on ice for 5–10 min, and pelleted for 2 min at full speed and 4°C. Total RNA was extracted from the cell pellets using the RNeasy Mini Kit (QIAGEN) according to the manufacturer's protocol, and genomic DNA was removed from the RNA samples (∼4 µg) using the TURBO DNA-free Kit (Invitrogen). RNA integrity was confirmed via agarose gel electrophoresis, RNA concentration was determined using a NanoDrop 1000 and Qubit fluorometer (RNA Broad-Range assay kit, Invitrogen), and cDNA was synthesized using ∼500 ng of each DNase-treated RNA sample and the High Capacity cDNA Reverse Transcription Kit (Applied Biosystems). M1 RNA (*rnpB*) transcript levels (Loveland et al. 2014) were measured via quantitative PCR (qPCR) using the resulting cDNA as template, PerfeCTa SYBR Green FastMix (Quantabio), and an Illumina Eco Real-Time PCR system. Primers targeting housekeeping genes *hcaT* and *cysG* were used as internal normalization controls (see Supplemental Table S4 for oligos used; Zhou et al. 2011). Reactions lacking reverse transcriptase were also used as template for qPCR to confirm the effective removal of genomic DNA. Data for each strain at each temperature are represented by three independent biological replicates, and qPCR was performed with three technical replicates for each biological replicate. To determine statistical significance, M1 RNA transcript levels from select A49 suppressor strains were compared to those of the DA61546 A49 parental strain at the corresponding temperature using a two-tailed Mann–Whitney test in GraphPad Prism. Values were considered significantly different if $P < 0.05$.

ASKA library screen

A plasmid library (representing 4000 cloned ORFs from *E. coli*) from ∼460,000 pooled clones from the ASKA collection (Kitagawa et al. 2006) was isolated using an EZNA Plasmid DNA Mini Kit I (Omega Bio-Tek). Electrocompetent *E. coli* A49 strain DA61546 cells were prepared as described previously, but with incubation at 30°C (Knopp et al. 2019), and ∼300 ng of the ASKA plasmid library or the empty pCA24N ASKA plasmid were transformed into 40 µL cells via electroporation. Cells were immediately recovered in 1 mL LB at 30°C with shaking at 190 rpm for 1 h. After incubation, a dilution series for each transformation was plated on LB-agar supplemented with 20 µg/mL chloramphenicol, which was then incubated overnight at 30°C, and the colonies were counted to determine the transformation efficiency and subsequently estimate the diversity of the library covered (∼10^6 total transformants). The remaining transformant recovery cultures were plated on LB-agar supplemented with 20 µg/mL chloramphenicol and 1 mM IPTG and allowed to incubate for ∼30 h at 42°C. Any colonies that appeared were restreaked on LB-agar supplemented with 20 µg/mL chloramphenicol and 1 mM IPTG and incubated overnight

at 42°C to confirm the rescue of the ts phenotype. Plasmids were isolated from these "positive hits" using the EZNA Plasmid DNA Mini Kit I (Omega Bio-Tek), sequenced using Sanger sequencing (Eurofins) to identify the cloned ORF recovered (Supplemental Table S4), retransformed into DA61546, and retested for growth at the nonpermissive temperature as described above.

SUPPLEMENTAL MATERIAL

Supplemental material is available for this article.

ACKNOWLEDGMENTS

This work was supported by grants from the Wallenberg Foundation (grant no. 2018.0168 to D.I.A.) and the Swedish Research Council (grant no. 2019-02091 to D.I.A.). The funders had no role in study design, data collection and analysis, decision to publish, or preparation of the manuscript. The quantitative proteomics analysis was performed by Evelin Berger at the Proteomics Core Facility, Sahlgrenska Academy, Gothenburg University, with financial support from SciLifeLab and BioMS. The authors thank Omar Mahmud Warsi and Hervé Nicoloff for their assistance with whole-genome sequencing and analysis, Roderich Römhild for help with growth curve analysis, and Nikolaos Fatsis-Kavalopoulos for help with data visualization and statistics. The thermometer image in Figure 3 is by vectorspoint from https://www.flaticon.com.

Received December 5, 2023; accepted April 12, 2024.

REFERENCES

Agrawal A, Mohanty BK, Kushner SR. 2014. Processing of the seven valine tRNAs in *Escherichia coli* involves novel features of RNase P. *Nucleic Acids Res* **42:** 11166–11179. doi:10.1093/nar/gku758

Altman S, Kirsebom LA. 1999. Ribonuclease P. In *The RNA world* (ed. Gesteland RF, Cech T, Atkins JF), pp. 351–380. Cold Spring Harbor Laboratory Press, Cold Spring Harbor, NY.

Andrade JM, Pobre V, Silva IJ, Domingues S, Arraiano CM. 2009. The role of 3′-5′ exoribonucleases in RNA degradation. *Prog Mol Biol Transl Sci* **85:** 187–229. doi:10.1016/S0079-6603(08)00805-2

Apirion D. 1980. Genetic mapping and some characterization of the *rnpA49* mutation of *Escherichia coli* that affects the RNA-processing enzyme ribonuclease P. *Genetics* **94:** 291–299. doi:10.1093/genetics/94.2.291

Baba T, Ara T, Hasegawa M, Takai Y, Okumura Y, Baba M, Datsenko KA, Tomita M, Wanner BL, Mori H. 2006. Construction of *Escherichia coli* K-12 in-frame, single-gene knockout mutants: the Keio collection. *Mol Syst Biol* **2:** 2006.0008. doi:10.1038/msb4100050

Baer MF, Wesolowski D, Altman S. 1989. Characterization *in vitro* of the defect in a temperature-sensitive mutant of the protein subunit of RNase P from *Escherichia coli*. *J Bacteriol* **171:** 6862–6866. doi:10.1128/jb.171.12.6862-6866.1989

Buck AH, Dalby AB, Poole AW, Kazantsev AV, Pace NR. 2005. Protein activation of a ribozyme: the role of bacterial RNase P protein. *EMBO J* **24:** 3360–3368. doi:10.1038/sj.emboj.7600805

Bush JW, Markovitz A. 1973. The genetic basis for mucoidy and radiation sensitivity. *Genetics* **74:** 215–225. doi:10.1093/genetics/74.2.215

Cairrão F, Cruz A, Mori H, Arraiano CM. 2003. Cold shock induction of RNase R and its role in the maturation of the quality control mediator SsrA/tmRNA. *Mol Microbiol* **50:** 1349–1360. doi:10.1046/j.1365-2958.2003.03766.x

Cheng I, Mikita N, Fishovitz J, Frase H, Wintrode P, Lee I. 2012. Identification of a region in the N-terminus of *Escherichia coli* Lon that affects ATPase, substrate translocation and proteolytic activity. *J Mol Biol* **418:** 208–225. doi:10.1016/j.jmb.2012.02.039

Condon C, Pellegrini O, Gilet L, Durand S, Braun F. 2021. Walking from *E. coli* to *B. subtilis*, one ribonuclease at a time. *C R Biol* **344:** 357–371. doi:10.5802/crbiol.70

Coughlin DJ, Pleiss JA, Walker SC, Whitworth GB, Engelke DR. 2008. Genome-wide search for yeast RNase P substrates reveals role in maturation of intron-encoded box C/D small nucleolar RNAs. *Proc Natl Acad Sci* **105:** 12218–12223. doi:10.1073/pnas.0801906105

Ebel W, Skinner MM, Dierksen KP, Scott JM, Trempy JE. 1999. A conserved domain in *Escherichia coli* Lon protease is involved in substrate discriminator activity. *J Bacteriol* **181:** 2236–2243. doi:10.1128/JB.181.7.2236-2243.1999

Ellis JC, Brown JW. 2009. The RNase P family. *RNA Biol* **6:** 362–369. doi:10.4161/rna.6.4.9241

El Mouali Y, Ponath F, Scharrer V, Wenner N, Hinton JCD, Vogel J. 2021. Scanning mutagenesis of RNA-binding protein ProQ reveals a quality control role for the Lon protease. *RNA* **27:** 1512–1527. doi:10.1261/rna.078954.121

Gillet-Markowska A, Louvel G, Fischer G. 2015. bz-rates: a web tool to estimate mutation rates from fluctuation analysis. *G3 (Bethesda)* **5:** 2323–2327. doi:10.1534/g3.115.019836

Größringer M, Far RKK, Hartmann RK. 2006. Analysis of RNase P protein (*mpA*) expression in *Bacillus subtilis* utilizing strains with suppressible *mpA* expression. *J Bacteriol* **188:** 6816–6823. doi:10.1128/JB.00756-06

Größringer M, Wäber NB, Wiegard JC, Hartmann RK. 2023. Characterization of RNA-based and protein-only RNases P from bacteria encoding both enzyme types. *RNA* **29:** 376–391. doi:10.1261/rna.079459.122

Grossman AD, Burgess RR, Walter W, Gross CA. 1983. Mutations in the Lon gene of *E. coli* K12 phenotypically suppress a mutation in the sigma subunit of RNA polymerase. *Cell* **32:** 151–159. doi:10.1016/0092-8674(83)90505-6

Guerrier-Takada C, Gardiner K, Marsh T, Pace N, Altman S. 1983. The RNA moiety of ribonuclease P is the catalytic subunit of the enzyme. *Cell* **35:** 849–857. doi:10.1016/0092-8674(83)90117-4

Gur E. 2013. The Lon AAA+ protease. In *Regulated proteolysis in microorganisms* (ed. Dougan DA), Vol. 66, pp. 35–51. Springer, New York.

Hamon A, Ycart B. 2012. Statistics for the Luria–Delbrück distribution. *Electron J Stat* **6:** 1251–1272. doi:10.1214/12-EJS711

Harris ME, Frank D, Pace NR. 1998. Structure and catalytic function of the bacterial ribonuclease P ribozyme. In *RNA structure and function* (ed. Simons RW, Grunberg-Manago M), pp. 309–337. Cold Spring Harbor Laboratory Press, Cold Spring Harbor, NY.

Hartmann RK, Größringer M, Späth B, Fischer S, Marchfelder A. 2009. The making of tRNAs and more—RNase P and tRNase Z. *Prog Mol Biol Transl Sci* **85:** 319–368. doi:10.1016/S0079-6603(08)00808-8

Henkels CH, Kurz JC, Fierke CA, Oas TG. 2001. Linked folding and anion binding of the *Bacillus subtilis* ribonuclease P protein. *Biochemistry* **40:** 2777–2789. doi:10.1021/bi002078y

Heuveling J, Possling A, Hengge R. 2008. A role for Lon protease in the control of the acid resistance genes of *Escherichia coli*. *Mol Microbiol* **69:** 534–547. doi:10.1111/j.1365-2958.2008.06306.x

Jain SK, Gurevitz M, Apirion D. 1982. A small RNA that complements mutants in the RNA processing enzyme ribonuclease P. *J Mol Biol* **162:** 515–533. doi:10.1016/0022-2836(82)90386-2

Jarrous N, Liu F. 2023. Human RNase P: overview of a ribonuclease of interrelated molecular networks and gene-targeting systems. *RNA* **29:** 300–307. doi:10.1261/rna.079475.122

Jovanovic M, Sanchez R, Altman S, Gopalan V. 2002. Elucidation of structure–function relationships in the protein subunit of bacterial RNase P using a genetic complementation approach. *Nucleic Acids Res* **30:** 5065–5073. doi:10.1093/nar/gkf670

Kazantsev AV, Pace NR. 2006. Bacterial RNase P: a new view of an ancient enzyme. *Nat Rev Microbiol* **4:** 729–740. doi:10.1038/nrmicro1491

Kim Y, Lee Y. 2009. Novel function of C5 protein as a metabolic stabilizer of M1 RNA. *FEBS Lett* **583:** 419–424. doi:10.1016/j.febslet.2008.12.040

Kim MS, Kim S, Kim SC, Lee YM, Jeon ES, Park CU, Lee Y. 1997. The *Brevibacterium albidum* gene encoding the arginine $tRNA_{CCG}$ complements the growth defect of an *Escherichia coli* strain carrying a thermosensitive mutation in the *rnpA* gene at the nonpermissive temperature. *Mol Gen Genet* **254:** 464–468. doi:10.1007/s004380050440

Kim MS, Park BH, Kim S, Lee YJ, Chung JH, Lee Y. 1998. Complementation of the growth defect of an *rnpA49* mutant of *Escherichia coli* by overexpression of arginine $tRNA_{CCG}$. *Biochem Mol Biol Int* **46:** 1153–1160.

Kim KS, Sim S, Ko JH, Lee Y. 2005. Processing of M1 RNA at the 3′ end protects its primary transcript from degradation. *J Biol Chem* **280:** 34667–34674. doi:10.1074/jbc.M505005200

Kirsebom LA, Trobro S. 2009. RNase P RNA-mediated cleavage. *IUBMB Life* **61:** 189–200. doi:10.1002/iub.160

Kirsebom LA, Baer MF, Altman S. 1988. Differential effects of mutations in the protein and RNA moieties of RNase P on the efficiency of suppression by various tRNA suppressors. *J Mol Biol* **204:** 879–888. doi:10.1016/0022-2836(88)90048-4

Kitagawa M, Ara T, Arifuzzaman M, Ioka-Nakamichi T, Inamoto E, Toyonaga H, Mori H. 2006. Complete set of ORF clones of *Escherichia coli* ASKA library (a complete set of *E. coli* K-12 ORF archive): unique resources for biological research. *DNA Res* **12:** 291–299. doi:10.1093/dnares/dsi012

Klemm BP, Wu N, Chen Y, Liu X, Kaitany KJ, Howard MJ, Fierke CA. 2016. The diversity of ribonuclease P: protein and RNA catalysts with analogous biological functions. *Biomolecules* **6:** 27. doi:10.3390/biom6020027

Knopp M, Gudmundsdottir JS, Nilsson T, König F, Warsi O, Rajer F, Ädelroth P, Andersson DI. 2019. De novo emergence of peptides that confer antibiotic resistance. *mBio* **10:** e00837-19. doi:10.1128/mBio.00837-19

Ko JH, Han K, Kim Y, Sim S, Kim KS, Lee SJ, Cho B, Lee K, Lee Y. 2008. Dual function of RNase E for control of M1 RNA biosynthesis in *Escherichia coli*. *Biochemistry* **47:** 762–770. doi:10.1021/bi701528j

Lai LB, Vioque A, Kirsebom LA, Gopalan V. 2010. Unexpected diversity of RNase P, an ancient tRNA processing enzyme: challenges and prospects. *FEBS Lett* **584:** 287–296. doi:10.1016/j.febslet.2009.11.048

Li Y, Cole K, Altman S. 2003. The effect of a single, temperature-sensitive mutation on global gene expression in *Escherichia coli*. *RNA* **9:** 518–532. doi:10.1261/rna.2198203

Li J, Van Vranken JG, Pontano Vaites L, Schweppe DK, Huttlin EL, Etienne C, Nandhikonda P, Viner R, Robitaille AM, Thompson AH, et al. 2020. TMTpro reagents: a set of isobaric labeling mass tags enables simultaneous proteome-wide measurements across 16 samples. *Nat Methods* **17:** 399–404. doi:10.1038/s41592-020-0781-4

Lin HC, Zhao J, Niland CN, Tran B, Jankowsky E, Harris ME. 2016. Analysis of the RNA binding specificity landscape of C5 protein reveals structure and sequence preferences that direct RNase P specificity. *Cell Chem Biol* **23:** 1271–1281. doi:10.1016/j.chembiol.2016.09.002

Loveland JL, Rice J, Turrini PCG, Lizotte-Waniewski M, Dorit RL. 2014. Essential is not irreplaceable: fitness dynamics of experimental *E. coli* RNase P RNA heterologous replacement. *J Mol Evol* **79:** 143–152. doi:10.1007/s00239-014-9646-8

Lundberg U, Altman S. 1995. Processing of the precursor to the catalytic RNA subunit of RNase P from *Escherichia coli*. *RNA* **1:** 327–334.

Meyer MM. 2017. The role of mRNA structure in bacterial translational regulation. *Wiley Interdiscip Rev RNA* **8:** 1–18. doi:10.1002/wrna.1370

Mohanty BK, Kushner SR. 2007. Ribonuclease P processes polycistronic tRNA transcripts in *Escherichia coli* independent of ribonuclease E. *Nucleic Acids Res* **35:** 7614–7625. doi:10.1093/nar/gkm917

Mohanty BK, Kushner SR. 2008. Rho-independent transcription terminators inhibit RNase P processing of the *secG leuU* and *metT* tRNA polycistronic transcripts in *Escherichia coli*. *Nucleic Acids Res* **36:** 364–375. doi:10.1093/nar/gkm991

Mohanty BK, Agrawal A, Kushner SR. 2020. Generation of pre-tRNAs from polycistronic operons is the essential function of RNase P in *Escherichia coli*. *Nucleic Acids Res* **48:** 2564–2578. doi:10.1093/nar/gkz1188

Morse DP, Schmidt FJ. 1992. Sequences encoding the protein and RNA components of ribonuclease P from *Streptomyces bikiniensis* var. *zorbonensis*. *Gene* **117:** 61–66. doi:10.1016/0378-1119(92)90490-G

Morse DP, Schmidt FJ. 1993. Suppression of loss-of-function mutations in *Escherichia coli* ribonucelase P RNA (M1 RNA) by a specific base-pair disruption. *J Mol Biol* **230:** 11–14. doi:10.1006/jmbi.1993.1120

Mosier AC, Li Z, Thomas BC, Hettich RL, Pan C, Banfield JF. 2015. Elevated temperature alters proteomic responses of individual organisms within a biofilm community. *ISME J* **9:** 180–194. doi:10.1038/ismej.2014.113

Motamedi H, Lee Y, Schmidt FJ. 1984. Tandem promoters preceding the gene for the M1 RNA component of *Escherichia coli* ribonuclease P. *Proc Natl Acad Sci* **81:** 3959–3963. doi:10.1073/pnas.81.13.3959

Nicoloff H, Andersson DI. 2013. Lon protease inactivation, or translocation of the *lon* gene, potentiate bacterial evolution to antibiotic resistance. *Mol Microbiol* **90:** 1233–1248. doi:10.1111/mmi.12429

Nicoloff H, Perreten V, Levy SB. 2007. Increased genome instability in *Escherichia coli lon* mutants: relation to emergence of multiple-antibiotic-resistant (Mar) mutants caused by insertion sequence elements and large tandem genomic amplifications. *Antimicrob Agents Chemother* **51:** 1293–1303. doi:10.1128/AAC.01128-06

Nicoloff H, Hjort K, Levin BR, Andersson DI. 2019. The high prevalence of antibiotic heteroresistance in pathogenic bacteria is mainly caused by gene amplification. *Nat Microbiol* **4:** 504–514. doi:10.1038/s41564-018-0342-0

Pascual A, Vioque A. 1996. Cloning, purification and characterization of the protein subunit of ribonuclease P from the cyanobacterium *Synechocystic* sp. PCC 6803. *Eur J Biochem* **241:** 17–24. doi:10.1111/j.1432-1033.1996.0017t.x

Paulo JA, O'Connell JD, Everley RA, O'Brien J, Gygi MA, Gygi SP. 2016. Quantitative mass spectrometry-based multiplexing compares the abundance of 5000 *S. cerevisiae* proteins across 10 carbon sources. *J Proteomics* **148:** 85–93. doi:10.1016/j.jprot.2016.07.005

Pereira C, Larsson J, Hjort K, Elf J, Andersson DI. 2021. The highly dynamic nature of bacterial heteroresistance impairs its clinical detection. *Commun Biol* **4:** 1–12. doi:10.1038/s42003-021-02052-x

Perez-Riverol Y, Csordas A, Bai J, Bernal-Llinares M, Hewapathirana S, Kundu DJ, Inuganti A, Griss J, Mayer G, Eisenacher M, et al. 2019. The PRIDE database and related tools and resources in 2019: improving support for quantification data. *Nucleic Acids Res* **47:** D442–D450. doi:10.1093/nar/gky1106

Phan HD, Lai LB, Zahurancik WJ, Gopalan V. 2021. The many faces of RNA-based RNase P, an RNA-world relic. *Trends Biochem Sci* **46:** 976–991. doi:10.1016/j.tibs.2021.07.005

Reams A, Roth JR. 2015. Mechanisms of gene duplication and amplification. *Cold Spring Harb Perspect Biol* **7:** a016592. doi:10.1101/cshperspect.a016592

Reich C, Olsen GJ, Pace B, Pace NR. 1988. Role of the protein moiety of ribonuclease P, a ribonucleoprotein enzyme. *Science* **239:** 178–181. doi:10.1126/science.3122322

SaiSree L, Reddy M, Gowrishankar J. 2001. IS186 insertion at a hot spot in the *lon* promoter as a basis for Lon protease deficiency of

Escherichia coli B: identification of a consensus target sequence for IS186 transposition. *J Bacteriol* **183:** 6943–6946. doi:10.1128/JB.183.23.6943-6946.2001

Sakamoto H, Kimura N, Nagawa F, Shimura Y. 1983. Nucleotide sequence and stability of the RNA component of RNase P from a temperature-sensitive mutant of *E. coli*. *Nucleic Acids Res* **11:** 8237–8251. doi:10.1093/nar/11.23.8237

Sakano H, Yamada S, Ikemura T, Shimura Y, Ozeki H. 1974. Temperature sensitive mutants of *Escherichia coli* for tRNA synthesis. *Nucleic Acids Res* **1:** 355–372. doi:10.1093/nar/1.3.355

Schedl P, Primakoff P. 1973. Mutants of *Escherichia coli* thermosensitive for the synthesis of transfer RNA. *Proc Natl Acad Sci* **70:** 2091–2095. doi:10.1073/pnas.70.7.2091

Son A, Choi S, Han G, Seong BL. 2015. M1 RNA is important for the in-cell solubility of its cognate C5 protein: implications for RNA-mediated protein folding. *RNA Biol* **12:** 1198–1208. doi:10.1080/15476286.2015.1096487

Sun L, Harris ME. 2007. Evidence that binding of C5 protein to P RNA enhances ribozyme catalysis by influencing active site metal ion affinity. *RNA* **13:** 1505–1515. doi:10.1261/rna.571007

Tallsjö A, Kirsebom LA. 1993. Product release is a rate-limiting step during cleavage by the catalytic RNA subunit of *Escherichia coli* RNase P. *Nucleic Acids Res* **21:** 1686. doi:10.1093/nar/21.7.1686-a

Thomason LC, Costantino N, Court DL. 2007. *E. coli* genome manipulation by P1 transduction. *Curr Protoc Mol Biol* **Chapter 1:** 1.17.1–1.17.8. doi:10.1002/0471142727.mb0117s79

Tlsty TD, Albertini AM, Miller JH. 1984. Gene amplification in the *lac* region of *E. coli*. *Cell* **37:** 217–224. doi:10.1016/0092-8674(84)90317-9

Tsilibaris V, Maenhaut-Michel G, Van Melderen L. 2006. Biological roles of the Lon ATP-dependent protease. *Res Microbiol* **157:** 701–713. doi:10.1016/j.resmic.2006.05.004

Van Melderen L, Aertsen A. 2009. Regulation and quality control by Lon-dependent proteolysis. *Res Microbiol* **160:** 645–651. doi:10.1016/j.resmic.2009.08.021

Vioque A, Arnez J, Altman S. 1988. Protein–RNA interactions in the RNase P holoenzyme from *Escherichia coli*. *J Mol Biol* **202:** 835–848. doi:10.1016/0022-2836(88)90562-1

Waugh DS, Pace NR. 1990. Complementation of an RNase P RNA (*rnpB*) gene deletion in *Escherichia coli* by homologous genes from distantly related eubacteria. *J Bacteriol* **172:** 6316–6322. doi:10.1128/jb.172.11.6316-6322.1990

Weber C, Hartig A, Hartmann RK, Rossmanith W. 2014. Playing RNase P evolution: swapping the RNA catalyst for a protein reveals functional uniformity of highly divergent enzyme forms. *PLoS Genet* **10:** e1004506. doi:10.1371/journal.pgen.1004506

Wegscheid B, Hartmann RK. 2006. The precursor tRNA 3′-CCA interaction with *Escherichia coli* RNase P RNA is essential for catalysis by RNase P in vivo. *RNA* **12:** 2135–2148. doi:10.1261/rna.188306

Wegscheid B, Hartmann RK. 2007. In vivo and *in vitro* investigation of bacterial type B RNase P interaction with tRNA 3′-CCA. *Nucleic Acids Res* **35:** 2060–2073. doi:10.1093/nar/gkm005

Wegscheid B, Condon C, Hartmann RK. 2006. Type A and B RNase P RNAs are interchangeable in vivo despite substantial biophysical differences. *EMBO Rep* **7:** 411–417. doi:10.1038/sj.embor.7400641

Wohlever ML, Baker TA, Sauer RT. 2013. A mutation in the N domain of *Escherichia coli lon* stabilizes dodecamers and selectively alters degradation of model substrates. *J Bacteriol* **195:** 5622–5628. doi:10.1128/JB.00886-13

Zecha J, Satpathy S, Kanashova T, Avanessian SC, Kane MH, Clauser KR, Mertins P, Carr SA, Kuster B. 2019. TMT labeling for the masses: a robust and cost-efficient, in-solution labeling approach. *Mol Cell Proteomics* **18:** 1468–1478. doi:10.1074/mcp.TIR119.001385

Zhou K, Zhou L, Lim Q, Zou R, Stephanopoulos G, Too HP. 2011. Novel reference genes for quantifying transcriptional responses of *Escherichia coli* to protein overexpression by quantitative PCR. *BMC Mol Biol* **12:** 18. doi:10.1186/1471-2199-12-18

MEET THE FIRST AUTHOR

Arianne M. Babina

***Meet the First Author(s)* is an editorial feature within *RNA*, in which the first author(s) of research-based papers in each issue have the opportunity to introduce themselves and their work to readers of *RNA* and the RNA research community. Arianne M. Babina is the first author of this paper, "Suppression of the *Escherichia coli rnpA49* conditionally lethal phenotype by different compensatory mutations." Arianne is a new Lecturer in Bacteriology in the School of Infection and Immunity at the University of Glasgow and an Affiliate Researcher in the Department of Medical Biochemistry and Microbiology at Uppsala University. Her research currently focuses on how bacterial genetic regulators (i.e., small proteins and noncoding RNAs) and subsequent regulatory networks arise de novo and evolve over time in response to environmental changes.**

What are the major results described in your paper and how do they impact this branch of the field?

Since the 1970s, complementation of the temperature-sensitive phenotype caused by the *rnpA49* mutant allele in *E. coli* has been an invaluable tool for investigating the biochemical and biophysical mechanisms underlying RNase P assembly and function. Although informative, previous studies often relied on the use of artificial approaches to examine complementation, including plasmid overexpression, gene deletion, and mutagenesis. As a result, there has been a knowledge gap regarding how *E. coli* naturally

Continued

suppresses the fitness defects resulting from the *rnpA49* mutation. In this study, we isolated and characterized naturally occurring second-site suppressor mutations of the temperature-sensitive phenotype in an *E. coli* strain carrying the *rnpA49* allele. Briefly, we found that *E. coli* can partially compensate for the *rnpA49* mutation via large genome amplifications of the regions encoding either subunit of the mutant RNase P complex (*rnpA49* or *rnpB*) or via loss-of-function mutations in RNase R or Lon protease. These findings agree with past plasmid overexpression studies and importantly suggest novel links between the A49 mutant RNase P and the regulatory pathways involving Lon protease and RNase R, a crucial step toward elucidating the many still unknown players and pathways involved in *E. coli* RNase P regulation. It is my hope this work paves the way for follow-up studies in the field, particularly those involving RNase P regulation, turnover, and degradation.

What led you to study RNA or this aspect of RNA science?

I was serendipitously introduced to the RNA field during an undergraduate research opportunity, after which I became fascinated by the many diverse and highly specialized biological roles of RNA, which go far beyond that of simply encoding proteins. Since then, I have been involved in a number of projects aimed at discovering and characterizing different RNAs and their interactions with various proteins and small molecules in a range of model organisms, including plants, archaea, and both Gram-negative and Gram-positive bacteria. The remarkable plasticity of RNA has further expanded my interests to include evolution and fitness, particularly within bacterial model systems. Wherever my science takes me, I always somehow manage to bring it back to RNA!

During the course of these experiments, were there any surprising results or particular difficulties that altered your thinking and subsequent focus?

The entire project was a bit of a surprise, actually. Despite *E. coli* A49's use in numerous studies over the course of many decades, it was surprising (and exciting!) that none of the *rnpA49* suppressor mutations we found were previously reported in the literature. Similarly, during a conversation with coauthor Leif Kirsebom about RNase P mutants, he mentioned that he occasionally came across a "slimy" looking *E. coli* A49 colony. It was really rewarding to eventually link that anecdotal observation to the mucoid Lon mutants that we now describe in this study.

Are there specific individuals or groups who have influenced your philosophy or approach to science?

I am forever grateful to Dieter Söll for giving me my first research opportunity as an undergraduate student and for introducing me to the field of "RNAs in bacteria." After a particularly frustrating week of experiments, he once told me "Science doesn't always work the way you want it to." Those reassuring words are still something I carry with me; I often think of them during a tough day in the laboratory, and I often find myself repeating them to colleagues and mentees in similar situations. It has become a mantra that both comforts and motivates me to continue moving forward in my research. Sure, it can be frustrating when something does not go as anticipated, but it is also the promise that things will not always work that encourages me to learn more, delve deeper, and become a better scientist.

Suppression of the *Escherichia coli rnpA49* conditionally lethal phenotype by different compensatory mutations

Arianne M. Babina, Leif A. Kirsebom and Dan I. Andersson

RNA 2024 30: 977-991 originally published online April 30, 2024
Access the most recent version at doi:10.1261/rna.079909.123